

1 Results and Discussion

1.1 Fiber Based Electrophysiology

(...)

1.1.1 Decomposition of Surface EMG Signals

Surface EMG recordings are a valuable tool to gain insights into the neuromuscular system. They are used, e.g., for the diagnosis of muscular disorders and in clinical studies that aim to advance biomedical understanding.

As described earlier, the EMG signals on the skin surface originate from the activated muscle fibers. Effects from volume conduction of action potentials on all muscle fibers are superpositioned and contribute to the EMG signal. The scaling of the contributions to the overall signal depends on several factors, such as the distance of the fibers to the skin surface. As all fibers in the same MU get activated simultaneously, each MU's contribution shows a characteristic “shape” in the resulting surface EMG signal. This shape is influenced by the number and location of the muscle fibers relative to the electrodes and the location of the neuromuscular junctions.

In our simulation, the location of the neuromuscular junctions is chosen pseudo-randomly (but deterministic) during initialization in the central 10 % of every muscle fiber. [Figure 1.1](#) shows the state of a simulation with 1369 fibers at $t = 1 \text{ ms}$, where all fibers have been activated at $t = 0 \text{ ms}$. The color coding indicates the potential V_m of the membrane, which at the shown time has only depolarized near the locations of the neuromuscular junctions.

Methods exist that seek to decompose the surface EMG signal into the contributions of the individual MUs. One popular method is *Gradient Convolution Kernel Compensation*

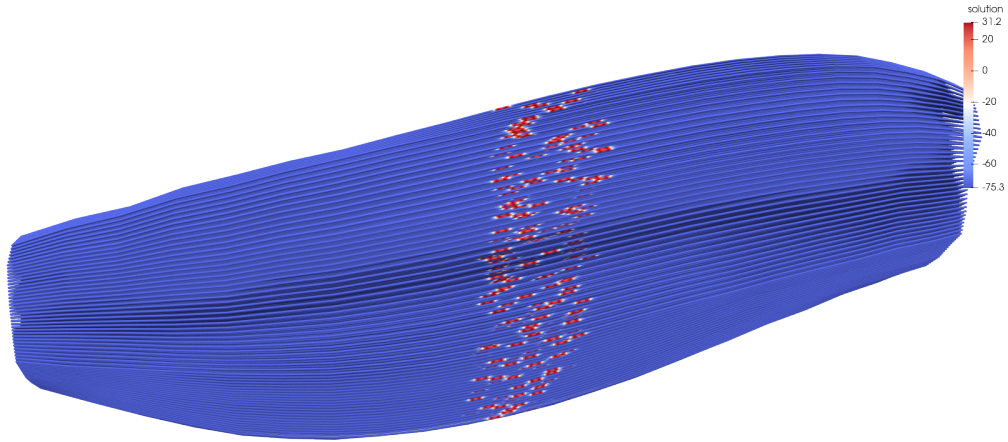


Figure 1.1: A simulation result that reveals the locations of the neuromuscular junctions. The figure depicts 1369 fibers after 1 ms that have initially been stimulated at the neuromuscular junction. The color coding corresponds to the membrane potential V_m , which has a positive value near the points of stimulation.

(gCKC) [Hol07a]; [Hol07b], which, in the following, will be outlined and then applied on simulated data.

Most decomposition methods, including the gCKC algorithm, assume that the EMG signal at an electrode is composed of the convolutional mixture of N filters of the MU activity. The activity of each MU $k \in \{1, \dots, N\}$ is described by the innervation pulse trains that activate the fibers of MU k , given as a point process of neural inputs at stimulation times φ_r . The source signal s_k in the muscle that represents the effect of MU k is described as a filter over these neural drives, $s_k(t) = \sum_r \delta(t - \varphi_r)$, where δ is the dirac delta function.

The vector of observed EMG values $\mathbf{x} \in \mathbb{R}^m$ at a time t is composed of the temporal convolution over L time-shifted sources \mathbf{s} and a term $\boldsymbol{\omega}$ of additive Gaussian noise:

$$\mathbf{x}(t) = \sum_{\ell=0}^{L-1} \mathbf{H}(\ell) \mathbf{s}(t - \ell) + \boldsymbol{\omega}(t).$$

Here, \mathbf{H} is the $m \times n$ mixing matrix for m observations and n MU sources and $\mathbf{s} = (s_k)_{1,\dots,n}$ is the vector of source signals. The sum over L previous values in this convulsive mixture can be reformulated by moving the summation into the matrix-vector product. The dimensions of the matrix \mathbf{H} and the vector \mathbf{s} are extended accordingly. Inversion of the extended mixture matrix yields the separation vectors, with which the innervation pulse trains φ_r of the MUs can be recovered from the recorded EMG signals \mathbf{x} . The gCKC algorithm performs the inversion indirectly by solving a derived optimization problem

using a gradient descent scheme.

The gCKC decomposition algorithm is implemented in the DEMUSE software, a commercial, MATLAB based tool that allows automatic and semi-automatic EMG decomposition [Hol08]. In collaboration with Lena Lehmann from the *Institute of Signal Processing and System Theory* and the *Institute for Modelling and Simulation of Biomechanical Systems*, we evaluated the performance of gCKC decomposition on simulated surface EMG signals.

We simulate fiber-based electrophysiology scenarios with fat layer and 1369 fibers using the same model parameter as in ???. In the first scenario, a fat layer with thickness of 1 cm is modelled. The simulated EMG signal is sampled in an electrode array with a frequency of 2 kHz and a grid size of 12×32 fibers, as shown in ??.

[Figure 1.2](#) shows the firing times of the 20 MUs in the first 10 s. The different MUs are initially activated every 100 ms to generate the shown “ramp” activation pattern, which later helps to identify the recovered MUs from the decomposition. From $t = 1.8$ s on, all MUs fire with their respective constant frequency, subject to jitter values of 10 %.

In this first scenario, the gCKC decomposition algorithm was applied on the first $t = 40$ s of simulated EMG data. The preconfigured algorithm in DEMUSE was used without manual intervention. While the simulated EMG recording consisted of an electrode grid of 12×32 fibers, only a rectangular subset of 5×13 channels at the lower center of the grid was used for the decomposition to mimic a realistic electrode array size. The DEMUSE software discarded four of these 65 channels as being invalid.

[Figure 1.2](#) shows the innervation pulses that were detected by DEMUSE as red vertical markers. A time span of 50 s was simulated of which only the first 11 s are visualized in [Fig. 1.2](#). DEMUSE found four MUs in this scenario, i.e., 20 % of the 20 simulated MUs. The recovered MUs were identified in the set of simulated MUs by matching the average firing frequency and the activation onset time in the ramp scheme. A first visual comparison with the original stimulation times given by the black markers shows a good agreement.

In this scenario, the association of fibers with MUs followed an exponential MU size progression with a basis of approximately 1.2, as shown in [Fig. 1.3a](#). The smallest MU contained two fibers and the largest MU had 256 fibers. The method 1 described in ?? was used to generate the association between fibers and MUs.

[Figure 1.3b](#) depicts the location of the four MUs that were detected by DEMUSE. The detected MUs have the indices 16, 18, 19 and 20 and correspond to four of the five largest MUs. It can be seen that MUs 18 to 20 are located mainly in the upper half of the muscle

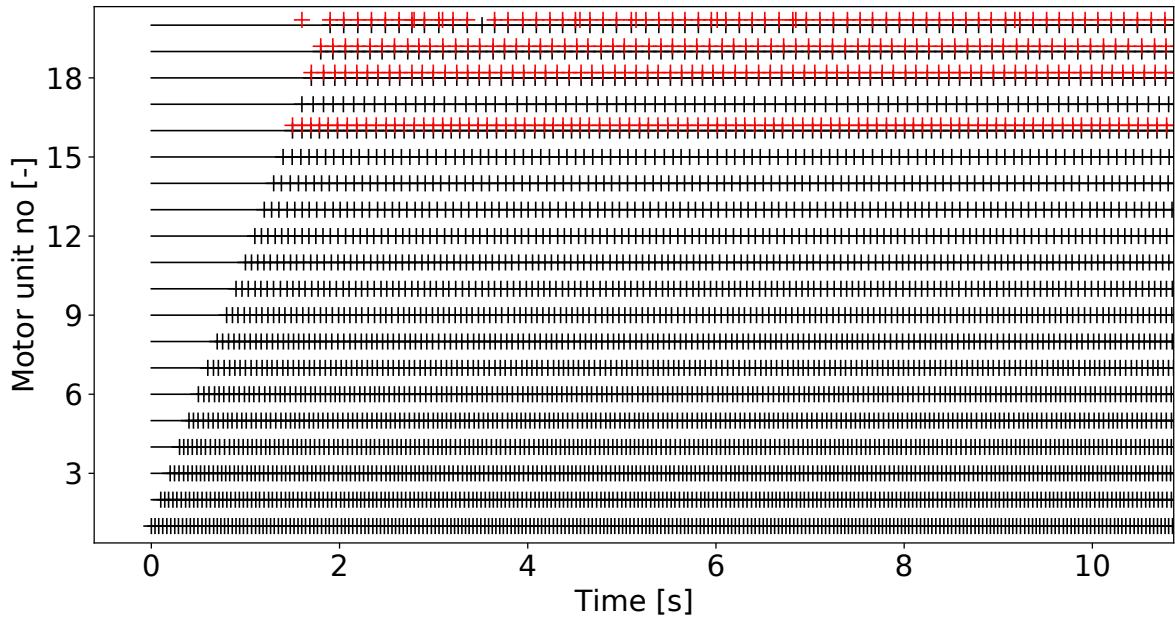


Figure 1.2: Match of EMG decomposition results with simulated data. The firing pattern over time for the 20 MUs in the simulation is shown by black markers. The recovered firing times of the gradient convolution kernel compensation algorithm are given by the red markers. The algorithm detected the four MUs 16, 18, 19 and 20.

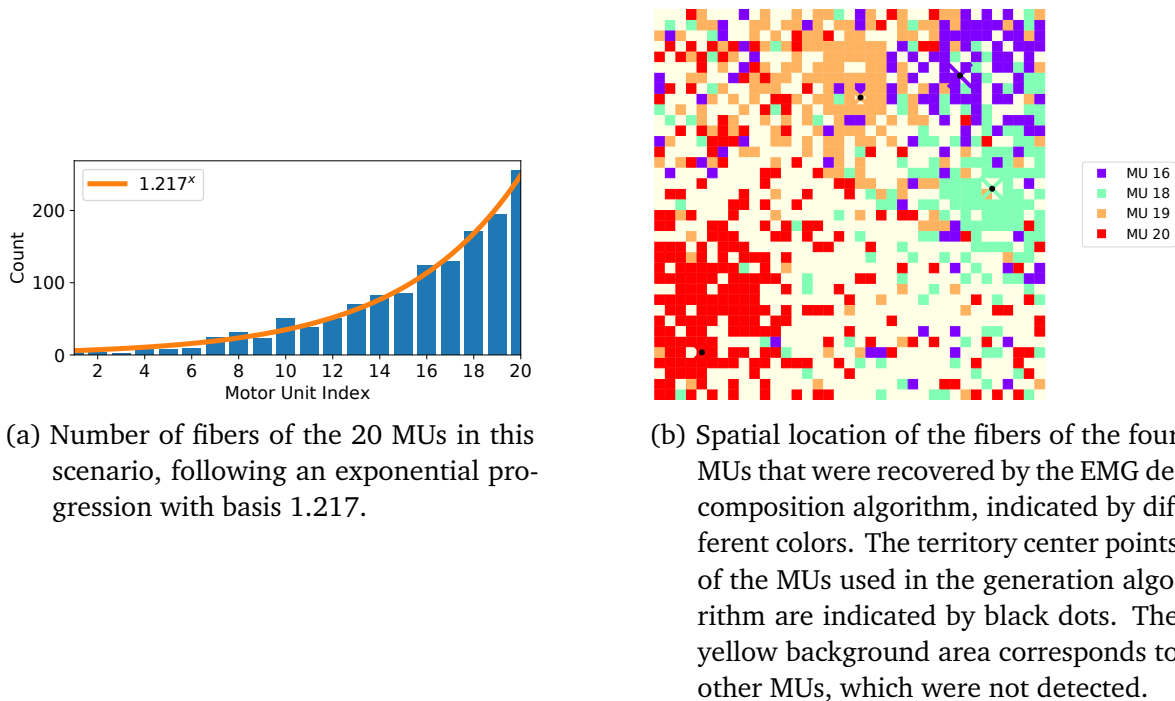


Figure 1.3: Association of the fibers with motor units for the first scenario with 20 MUs, given in Fig. 1.2.

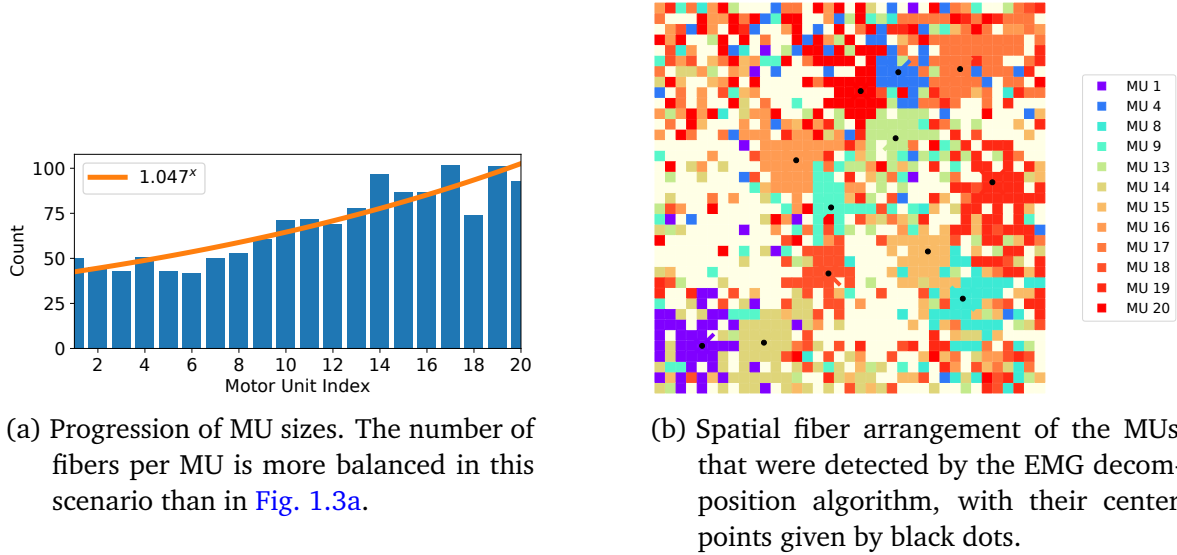


Figure 1.4: Association of the fibers with motor units for the second scenario with 20 MUs, given in Fig. 1.5.

cross-section, in proximity to the electrode array at the top of the diagram. The MU with the most fibers, MU 20, was detected by the decomposition algorithm even though it is located at the lower left of diagram at a large distance to the skin surface.

Two further scenario were simulated with the same parameters as the first scenario in Fig. 1.2, but instead with 50 and 100 MUs. In these datasets, DEMUSE was able to detect 8 and 12 MUs, which corresponds to 16 % and 12 %.

Moreover, another scenario with 20 MUs was computed, but the fat layer was varied to have a thickness of only 2 mm instead of 1 cm. In addition, the association scheme between MUs and fibers was changed to the one shown in Fig. 1.4. The exponential distribution of MU sizes only varied between 42 and 102 fibers per MU, corresponding to a basis in the exponential function of approximately 1.05 instead of 1.2.

Figure 1.5 shows the results of the EMG decomposition with the gCKC algorithm for this second scenario with 20 MUs. DEMUSE successfully decomposed the signal into 13 MUs, corresponding to 65 % of the 20 simulated MUs. DEMUSE also determined two additional MUs, which we do not consider part of the set of successfully recovered MUs. The first dataset only consists of ten innervation pulses, and the second pulse train contains high frequency oscillations. In this scenario, the software marked only one EMG recording channel as invalid, which means that more data was considered by the decomposition algorithm than in the first scenario with 20 MUs.

Similar to the previously presented scenario, the larger MUs were detected with a

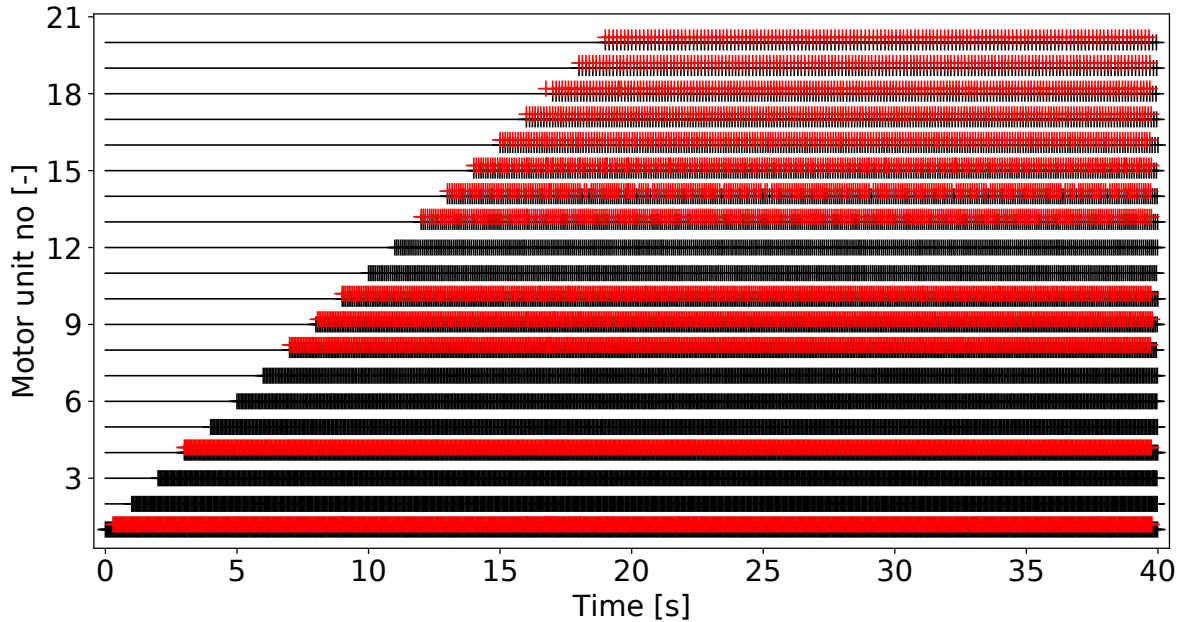
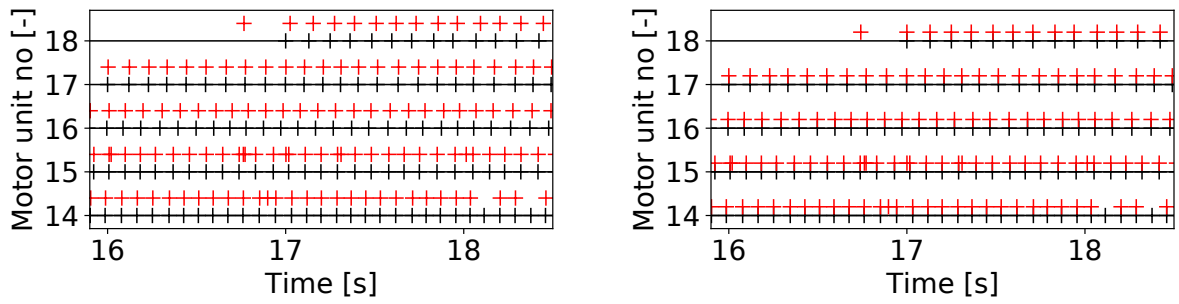


Figure 1.5: Activation pattern for the second scenario with 20 MUs. The activation times used in the simulation are shown as black markers, the recovered activation pulses of the EMG decomposition algorithm are shown as red markers.



(a) Original data where a constant time shift between the simulated (black) and recovered (red) markers can be seen, especially for MUs 16 and 18.

(b) Same data as in (a) with applied time offset correction. The applied time shifts for MUs 16 and 18 are -12.9 ms and -24.9 ms , respectively.

Figure 1.6: Excerpts of the detected firing times of MUs 14 to 18 in the second scenario with 20MUs. The stimulation times of the simulation are given by black markers, the recovered times are visualized by red crosses.

higher probability than the smaller MUs. In this scenario, the eight largest MUs were successfully found. [Figure 1.4b](#) shows the spatial arrangement of the detected MUs. The area of the muscle cross section that is occupied by undetected MUs is again distributed more distantly to the skin surface at the upper boundary. However, the recovered MUs 1 and 14 are nevertheless located at the lower boundary, i.e., in the most distant area from the EMG electrodes.

Next, we evaluate the quality of the innervation pulse trains that were recovered by the gCKC algorithm in our scenarios. We compare the stimulation times calculated by DEMUSE with the stimulation times of the simulation. [Figure 1.6a](#) shows an excerpt of the detected pulse trains of the second scenario with 20 MUs in [Fig. 1.5](#), where the gCKC algorithm recovered 13 MUs. We observe for some MUs that the recovered stimulation times are consistently shifted in time. This effect is especially visible for MUs 16 and 18.

The reference times given by the black markers in [Fig. 1.6a](#) correspond to the times when the fibers were stimulated in the simulation in OpenDiHu. The detected MU activations in DEMUSE, however, correspond to the times when the MU action potential shapes in the EMG recording reached their maximum. Moreover, the exact times when particular MUs reach particular EMG electrodes depend on the distance of the electrodes to the innervation points of the MUs. The further the electrodes are away from the neuromuscular junctions along the muscle, the higher is the delay of the recorded spikes to the corresponding innervation pulses. Thus, the constant time shifts in the pulses detected by the gCKC algorithm are valid and have to be accounted for in the evaluation of the decomposition performance.

We correct for these time shifts by adding constant time offsets Δt_k to the recovered innervation pulse trains. For every MU k , the algorithm finds the matching pairs of simulated and recovered pulses and optimizes the value of Δt_k such that the time differences in these pairs after shift correction get minimal.

[Figure 1.6b](#) shows the same extract of MU activity as in [Fig. 1.6a](#) with applied time offsets. The time offsets for MUs 14 to 18 in this example are given as

$$\begin{aligned}\Delta t_{14} &= -2.4 \text{ ms}, & \Delta t_{15} &= -1.1 \text{ ms}, & \Delta t_{16} &= -12.9 \text{ ms}, \\ \Delta t_{17} &= -2.9 \text{ ms}, \quad \text{and} & \Delta t_{18} &= -24.9 \text{ ms}.\end{aligned}$$

[Figure 1.6b](#) shows that the recovered pulses now match the simulated data very well. The non-matching pulses are clearly false positive detections.

To compare the recovered MU times between the scenarios, we evaluate metrics such as the rate of agreement. The MU firing times in the simulation serve as the ground truth to which we compare the recovered MU times. We identify true positive (TP), false positive (FP) and false negative (FN) recovered pulses, depending on whether a matching time to a recovered pulse can or cannot be found in the simulation data within a tolerance of $\varepsilon = 5 \text{ ms}$. The rate of agreement (RoA) between the gCKC algorithm output and the

ground truth data is then computed by

$$\text{RoA} = \frac{\text{TP}}{\text{TP} + \text{FP} + \text{FN}}.$$

In the first scenario with 20 MUs in [Fig. 1.2](#), the RoA for MUs 16, 18 and 19 is above 99.7% and slightly lower at 82.2% for MU 20. Here, only 296 of the 334 detected pulses were true positives, corresponding to a precision of 88.6%.

In the second scenario with 20 MUS presented in [Fig. 1.5](#), all valid MUs except one have RoA values of above 94.5 %. Five MUs are even detected perfectly with 100 % rate of agreement. MU 9 is the only detected MU with a degraded RoA of approximately 57.9 %. However, the RoA improves to 98.1 %, if the tolerance ϵ for matching pulses is relaxed to 10 ms. This shows that the RoA metric also depends on a proper value for the tolerance ϵ , and that some of the innervation pulse trains detected by DEMUSE can have varying accuracy in a range of less than 10 ms.

While the gCKC algorithm can be used for EMG decomposition of previously recorded signals in a controlled environment, it is less suited for real-time applications such as human-machine interfaces (HMI). The separation vectors that decompose the electrode signals and infer the MU innervation pulse trains can be computed in a training phase. However, their application on new data requires a certain history of previously captured signals to calculate the decomposed MU pulses. In consequence, the predictions are delayed, which is usually undesirable in HMI applications. Furthermore, the system is sensitive to noisy data.

A fundamentally different approach to EMG decomposition is the use of sequence-to-sequence learning methods provided by recurrent neural networks. The authors of [\[Cla21\]](#) used a gated recurrent unit (GRU) network for this task. The network was trained using the output of the gCKC algorithm and was subsequently able to decompose surface EMG signals into innervation pulse trains. The approach was shown to be robust and to outperform gCKC for low signal-to-noise ratios.

To assess, whether our simulations of surface EMG can be used for the supervised learning of GRU networks for EMG decomposition, we tried in a first step to reproduce the studies of [\[Cla21\]](#), where the GRU is trained with the output of the gCKC algorithm. Additionally, we trained a GRU network directly on the simulated EMG data. These tasks were carried out in the masters project of Srijay Kolvekar and were supervised by Lena Lehmann and me. For details on the methods and results, we refer to the literature [\[Cla21\]](#) and the project report [\[Kol21\]](#).

In this project, the EMG decomposition of a GRU network trained with raw innervation pulse trains obtained from the gCKC algorithm, similar to the literature, showed a large number of false positive and false negative predictions. However, a different setup using MU labels instead of raw pulse trains showed promising results. Every discrete point in time (according to the EMG sampling frequency) was either associated with the class of the currently active MU or with the background class, when no MU was activated at the time. This classification problem had a large class imbalance, as the background class was active for 86 % of the timesteps. The issue was mitigated by using class weights. The GRU network was trained with simulation data and yielded per-class rates of agreement of up to 72 % for the two scenarios with 20 MUs shown in [Figures 1.2](#) and [1.5](#).

[Figure 1.7](#) presents an excerpt of the resulting predictions of a GRU network that was trained with simulation results. We used the simulation of the second scenario with 20 MUs, which is shown in [Fig. 1.5](#). The black markers in [Fig. 1.7](#) indicate the stimulation times used in the simulation. The red markers correspond to the recovered times by the gCKC algorithm. Out of the shown MUs, only MUS 9 and 10 were recovered by the gCKC algorithm. The blue markers denote the GRU predictions. Correction of time offsets was performed for both the gCKC and GRU outputs.

[Figure 1.7](#) shows the best agreement between the two prediction methods for MU 10 with a RoA of 99.6 % for the gCKC algorithm and 72.2 % for the GRU network. In contrast to the gCKC algorithm, the GRU network predicts firings for all MUs. However, the quality is only acceptable for MUs that could also be detected by the gCKC algorithm. For MUs 11 and 12, the RoA for the GRU network is around 30 %.

In future work, the decomposition performance of the GRU networks could be improved by using different training data. For example, the ramp activation in the training data could be replaced by constant tetanic stimulations or training data where different single MUs are activated at a time could be investigated.

In conclusion, the gCKC algorithm is able to decompose artificially generated surface EMG signals. This means that our simulation can be used to evaluate the performance of EMG decomposition algorithms.

The number of detected MUs depends on the relation between MU sizes and on the distance of the MU territories to the electrodes. If the variance of the sizes of the activate MUs is small, such as in [Fig. 1.4a](#), also MU are detected that are far away from the electrodes. If, in the opposite case, the sizes of active MUs are distributed over a large range such as in [Fig. 1.3a](#), only the largest MUs are detectable.

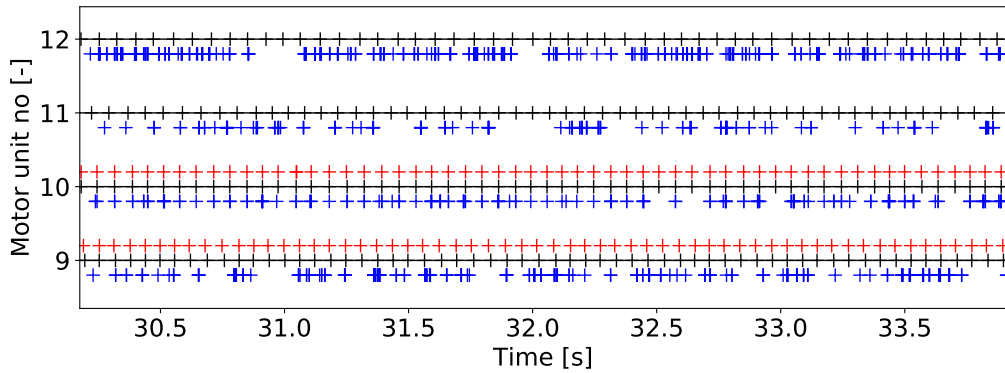


Figure 1.7: Comparison of innervation pulse train predictions of the gCKC algorithm (red), a GRU network (blue) and the ground truth data (black).

In addition, the amount of adipose tissue between the electrodes and the muscle influences the number of MUs that can be recovered. In our studies, the performance of EMG decomposition was lower for all scenarios with thicker fat layer than for the scenario with a thin fat layer.

The rate of agreement of the determined pulse trains of the DEMUSE software was above 95 % in most of the cases. Correspondingly, the rate of false positives was low. A time shift between the recovered times and the ground truth data was observed for some pulse trains, however, it can be explained with the delay from first activation to the onset of the EMG signal. As a result, the time shift was corrected for the rate of agreement measurement.

A proof-of-concept implementation of GRU networks showed promising performance for predicting MU firing times from artifical EMG recordings. In future work, the algorithm has to be refined to be comparative to the gCKC algorithm.

Bibliography

- [Cla21] **Clarke**, A. K. et al.: *Deep learning for robust decomposition of high-density surface emg signals*, IEEE Transactions on Biomedical Engineering 68.2, 2021, pp. 526–534, [doi:10.1109/TBME.2020.3006508](https://doi.org/10.1109/TBME.2020.3006508)
- [Hol07a] **Holobar**, A.; **Zazula**, D.: *Multichannel blind source separation using convolution kernel compensation*, IEEE Transactions on Signal Processing 55.9, 2007, pp. 4487–4496, [doi:10.1109/TSP.2007.896108](https://doi.org/10.1109/TSP.2007.896108)
- [Hol07b] **Holobar**, A.; **Zazula**, D.: *Gradient convolution kernel compensation applied to surface electromyograms*, Independent Component Analysis and Signal Separation, ed. by **Davies**, M. E. et al., Berlin, Heidelberg: Springer Berlin Heidelberg, 2007, pp. 617–624, isbn:978-3-540-74494-8
- [Hol08] **Holobar**, A.; **Zazula**, D.; **Merletti**, R.: *Demusetool-a tool for decomposition of multi-channel surface electromyograms*, 2008
- [Kol21] **Kolvekar**, S.: *Gated Recurrent Unit Network for Decomposition of Synthetic High-Density Surface Electromyography Signals*, MA thesis, Pfaffenwaldring 47, 70569 Stuttgart, Germany: Institute for Signal Processing and System Theory, University of Stuttgart, 2021